

The Effect of Incorporation of Ferrite Nanoparticles on Compressive Strength and Resistivity of Self-Compacting Concrete

Mohamed A. Ahmed^{1*}, Yehia A. Hassanean², Kamal A. Assaf², Moustafa A. Shawkey¹

¹Materials Science Lab. (1), Physics Department, Faculty of Science, Cairo University, Giza, Egypt

²Department of Civil Engineering, Assiut University, Assiut, Egypt

Email: *moala47@hotmail.com

Received 22 February 2015; accepted 12 March 2015; published 17 March 2015

Copyright © 2015 by authors and Scientific Research Publishing Inc.

This work is licensed under the Creative Commons Attribution International License (CC BY).

<http://creativecommons.org/licenses/by/4.0/>



Open Access

Abstract

Mn-Ferrite nanoparticles were prepared using citrate auto combustion method. The prepared sample was characterized by X-ray diffraction (XRD), HRTEM and BET to measure the particle diameter and the surface area of the prepared sample. The data of XRD clarified that the sample was formed in single phase spinel structure without any extra peaks indicating non-existence of any secondary phase. The HRTEM micrograph indicated that the particles were in an agglomerated state due to the absence of surfactant and high magnetic properties of Mn-Ferrite nanoparticles. The mechanical properties were measured at different ratios of nano-Ferrite to concrete. The obtained values of mercury intrusion porosimetry (MIP) indicated that the addition of Mn-Ferrite nanoparticles increased the compressive strength and decreased the total intrusion volume. This was due to the rapid consuming of $\text{Ca}(\text{OH})_2$ which was formed during hydration of Portland cement especially at early ages due to the high reactivity of MnFe_2O_4 nanoparticles. Moreover, MnFe_2O_4 nanoparticles recovered the particle packing density of the blended cement, leading to a reduced volume of pores in the cement paste.

Keywords

Compressive Strength, Concrete, XRD, HRTEM, Reactivity

1. Introduction

Concrete is the most commonly and widely used as construction material in the entire world. It is actually

*Corresponding author.

unique in construction as it is the only material exclusive to the business and therefore is the beneficiary of a fair proportion of the research and development money from industry [1]. Self compacting concretes (SCCs) are characterized by high packing densities which can be achieved with enhancement of grain size distribution by incorporating a homogeneous gradient of fine and coarse particles leading to improvement in the concrete mix [2] [3].

The understanding of the structure and behavior of concrete at the fundamental stage is a necessary and very appropriate use of nanotechnology. One of the fundamental aspects of nanotechnology is its interdisciplinary nature [1]. Concrete is a macro-material strongly influenced by its nano-properties and understanding it at this new level is opening new era for improvement the mechanical properties of concrete [4].

However, one of the advantages made by the study of concrete at the nanoscale is that particle packing in concrete can be improved by using MnFe_2O_4 nanoparticles leading to an enhancement of densification of the micro and nanostructure resulting in improved mechanical properties. MnFe_2O_4 nanoparticles addition to cement based materials can also control the formation of the fundamental calcium silicate hydrate (C-S-H) reaction of concrete caused by calcium leaching in water as well as block water penetration and therefore lead to improvements in durability [5].

Previously, several works have been conducted on concrete composites by adding different nanoparticles evaluating the mechanical properties of concrete. The activity of nanoparticles can act as heterogeneous nuclei for cement pastes, further accelerating cement hydration, as nanoreinforcement, and as nano filler, densifying the microstructure, leading to a reduced porosity [6].

The aim of this study is incorporating MnFe_2O_4 nanoparticles into SCCs to examine compressive strength of self-compacting concrete. In addition, pore structure and microstructure of the concrete specimens will be evaluated. Several specimens with a constant amount of polycarboxylate superplasticizer (PC) will be prepared and their physical and mechanical properties will be measured for different partial substitutions of MnFe_2O_4 nanoparticles to the cement paste [7].

When Ferrite nanoparticles are added to cement/concrete, they act as filler to fill the pores between cement particles resulting in finer pore structure. Also, more C-S-H gel can be formed in concrete due to the reaction that occurs between the Ferrite nanoparticles and the $\text{Ca}(\text{OH})_2$ in the hydrating of cement [8].

MnFe_2O_4 nanoparticles have been found to improve compressive strength of concrete, to increase resistance of failure and turn control the leaching of calcium, in addition, promote the hydration reactions of tricalcium silicate (C_3S) as a result of the large and highly reactive surface of the nanoparticles [4].

Addition of 0.5% MnFe_2O_4 nanoparticles with dispersing agents has been observed to increase the compressive strength of concrete composites after 28 days by as much as 22%.

2. Materials and Methods

2.1. Materials and Mixtures

2.1.1. Cement

Ordinary Portland Cement (OPC) grade (CEM I 52.5N) obtained from AL-Areash Cement Manufacturing Company of Egypt conforming to the British standard BS 12/1996 [9] was used as received. The chemical properties of the cement are obtained from Analytical Axios Advanced X-ray fluorescence (XRF) and the results are reported in **Table 1**.

2.1.2. MnFe_2O_4 Nanoparticles

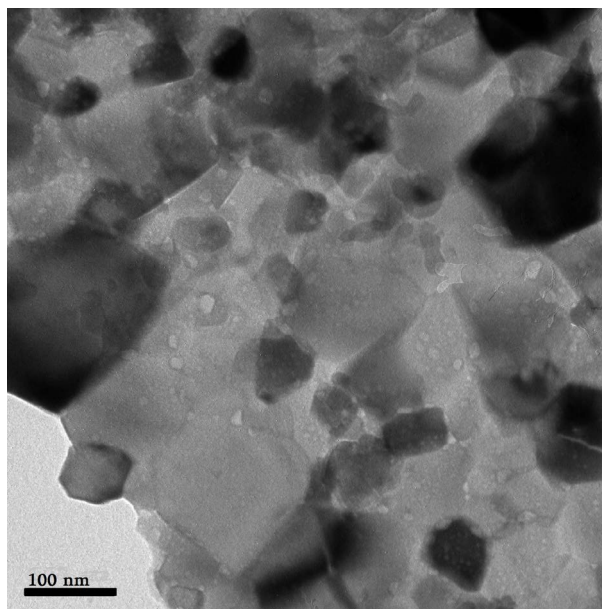
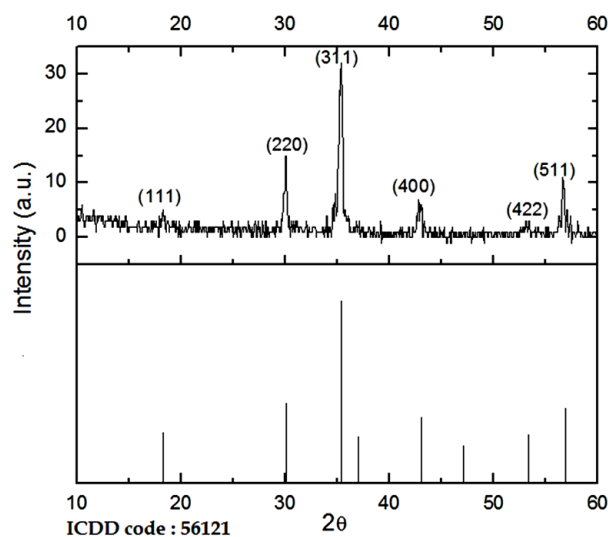
MnFe_2O_4 nanoparticles with average diameter of 49 nm and average surface area of $27.28 \text{ m}^2/\text{g}$ was prepared by citrate nitrate auto combustion method at Materials Science Lab. (1) [10] [11]. The properties of MnFe_2O_4 nanoparticles are shown in **Table 2**. High-resolution transmission electron microscopy (HRTEM) and powder X-ray diffraction (XRD) diagrams of MnFe_2O_4 nanoparticles are shown in **Figure 1** and **Figure 2**, respectively.

Table 1. Properties of Portland cement (wt%).

Al_2O_3	SiO_2	CaO	TiO_2	Na_2O	MgO	SO_3	K_2O	Fe_2O_3	L.O.I
4.46	15.15	66.89	0.37	0.58	0.58	4.02	0.22	4.49	3.24

Table 2. Properties of MnFe₂O₄ nanoparticles.

Average diameter/nm	Average surface area/(m ² /g)	Average volume/(cc/g)	Purity/%
49	27.28	0.0134	98 - 99

**Figure 1.** HRTEM micrograph of MnFe₂O₄ nanoparticles.**Figure 2.** XRD analysis of MnFe₂O₄ nanoparticles.

2.1.3. Aggregates

Crushed limestone aggregates (4.75 - 12.5 mm) were used to produce self-compacting concretes, with gravel (12.5 - 22 mm) and coarse sand (0.5 - 2 mm).

2.1.4. Superplasticizer

Sika ViscoCrete[®]-5930 is an aqueous solution of modified polycarboxylate was used. **Table 3** reports some of the physical and chemical properties of polycarboxylate admixture used in this study.

Table 3. Physical and chemical characteristics of the superplasticizer admixture.

Appearance	Colour	Specific gravity/(kg/L)	Na ⁺ Ppm	Ca ⁺ Ppm
Turbid liquid	Yellow-brown	1.08 ± 0.005	18380	4.72

2.1.5. Mixture Proportioning

Two series of mixtures were prepared in the laboratory trials as shown in **Table 4**. C0-SCC mixtures were prepared as control specimens. The control mixtures were made of natural aggregates, cement and water. N series were prepared with different concentrations of MnFe₂O₄ nanoparticles with average diameter of 49 nm. The mixtures were prepared with the nanoparticles replacement of 0.5%, 1.0%, 1.5% and 2.0% by weight of cement and 0.5 wt% polycarboxylate admixture. The superplasticizer was dissolved in water, and then the MnFe₂O₄ nanoparticles were added and good stirred at a high speed for 2 min. The aggregates for the mixtures consisted of a combination of Crushed limestone, gravel and sand. The binder content of all mixtures was 650 kg/m³. The total mixing time including homogenizing was 5 minutes.

2.2. Strength Evaluation Tests

Cubic specimens with 100 mm edge length were used for compressive tests [5]. The moulds were covered with polyethylene sheets and moistened for 24 h. Then the specimens were demoulded and cured in water at room temperature prior to test days [4]. The strength tests of the specimens were determined after 7 and 28 days of curing. Compressive tests were carried out according to the ASTM C 39 [12] standard. The tests were carried out triplicately and average strength values were obtained.

2.3. Mercury Intrusion Porosimetry (MIP)

MIP Poresizer 9320 V2.08 was used to characterize the pore structure in porous material as a result of its simplicity, quickness and wide measuring range of pore diameter [13] [14]. MIP gives us details about the dimensions of pores [13]. To prepare the specimens for MIP measurement, the concrete specimens after 28 days of curing were first broken into smaller pieces, and then the cement paste fragments selected from the center of prisms were used to measure pore structure. The specimens were immersed in acetone to stop hydration as fast as possible. Before mercury intrusion test, the specimens were dried in an oven at about 110°C until constant weight is obtained by removing moisture in the pores. MIP is based on the assumption that the non wetting liquid mercury (the contact angle between mercury and solid is greater than 90°) will only intrude in the pores of porous material under pressure [13] [14]. Each pore size is quantitatively determined from the relationship between the volume of intruded mercury and the applied pressure [11]. The test apparatus used for pore structure measurement is Auto Pore III mercury porosimeter. The surface tension of mercury is taken as 485 × 10⁻⁵ N/cm (485 dyne/cm), and the contact angle selected is 130 deg. The maximum head pressure applied is (4.68 psi).

2.4. Thermogravimetric Analysis (TGA) and Derivative Thermogravimetry (DTG)

A Netzsch STA 409 simultaneous thermal analyzer was used to measure the weight loss of the specimens. Specimens which were cured for 28 days were heated to 650°C, at a heating rate of 4°C/min and in an inert N₂ atmosphere.

2.5. Scanning Electron Microscopy (SEM)

SEM investigations were conducted on a Hitachi Model S-3700N CD-SEM apparatus. Backscattered electron (BSE) and secondary electron (SE) imaging was used to study the specimens, which were prepared under conditions that ensured their subsequent viability for analytical purposes.

3. Results and Discussion

Table 5 shows the compressive strength of C0-SCC and N-SCC specimens after 7 and 28 days of curing. The results show that the compressive strength increases by adding MnFe₂O₄ nanoparticles by 0.5 wt% replacements and then it decreases. MnFe₂O₄ nanoparticles accelerate consumption of crystalline Ca(OH)₂ which quickly are

Table 4. Mix proportion of samples.

Sample name	MnFe ₂ O ₄ nanoparticles/%	SP content /%	Quantities/(kg/m ³)						
			Water	SP	Sand	Gravel	Crushed limestone	Cement	MnFe ₂ O ₄ nanoparticles
C0	0	0.5	180	3.25	580	580	580	650	0
N1	0.5	0.5	180	3.25	580	580	580	646.75	3.25
N2	1	0.5	180	3.25	580	580	580	643.5	6.5
N3	1.5	0.5	180	3.25	580	580	580	640.25	9.75
N4	2	0.5	180	3.25	580	580	580	637	13

Table 5. Compressive strength of C0-SCC and N-SCC specimens.

Sample name	MnFe ₂ O ₄ nanoparticles/%	Compressive strength/MPa 7 days	Compressive strength/MPa 28 days
C0	0	52.7	56.4
N1	0.5	65.3	68.9
N2	1	62.6	64.3
N3	1.5	51.5	56.3
N4	2	49.2	68.9

formed into C-S-H during hydration of cement specially at early ages due to the high reactivity of these nanoparticles. As a consequence, larger volumes of reaction products are formed. Moreover, MnFe₂O₄ nanoparticles act as filler for strengthening the micro structure of cement. They reduce the quantity and size of Ca(OH)₂ crystals and fill the voids of C-S-H gel structure to make the structure of hydrated product more compact [15].

However, increasing MnFe₂O₄ nanoparticles more than 0.5 wt%, the compressive strength reduces. This is because the amount of MnFe₂O₄ nanoparticles present in the mix is higher than the amount required to combine with the liberated lime during the process of hydration. This leads to an excess of silica leaching out and causes degradation in strength. Though, nanoparticles replace part of the cementitious material but don't contribute in the reaction. Also, cracks generated in dispersion of nanoparticles cause weak zones [16] [17].

In other words, this phenomenon can be explained by the assumption that nanoparticles are uniformly distributed in concrete and each particle is contained in a cube pattern. Therefore, the distance between nanoparticles can be determined. After the beginning of hydration process, hydrate products diffuse and envelop nanoparticles as kernel [6] [15].

When the amount of nanoparticles and the distances between them are appropriate, they can accelerate C-S-H gel formation as a result of increased crystalline Ca(OH)₂ amount at the early age of hydration due to their high reactivity, and hence the compressive strength of concrete increases. With excessive increase of MnFe₂O₄ nanoparticles, the distance between them decreases and Ca(OH)₂ crystals required for C-S-H gel formation don't grow up enough due to limited space and therefore, the formation of Ca(OH)₂ crystals is hindered. The result of this process is the increase in shrinkage and creep of concrete mix and decreasing the compressive strength [6].

The mercury intrusion results of the C0-SCC specimen and N1-SCC specimen are shown in **Figure 3** and **Figure 4**. **Figure 3** represents the variation of incremental intrusion, reflecting pore volume against pore diameter, which indicates that most pore diameter of the specimen are distributed between 0.1 micrometer to 1 micrometer. **Figure 4** represents the cumulative intrusion, reflecting the total connected pore volume of pore sizes. **Table 6** shows that by increasing MnFe₂O₄ nanoparticles by 0.5 wt%, total intrusion volume of specimens of concrete are decreased. This leads to decreasing total pore area and median pore diameter (area), but median pore diameter (volume) of these specimens is increased.

On the other hand, **Table 7** shows that the addition of MnFe₂O₄ nanoparticles by 0.5 wt% leads to decreasing the porosity, increase the average pore diameter and decreasing the bulk density and the apparent (skeletal) density of these specimens of concrete. This means the regularity of porosity is similar to that of total intrusion vo-

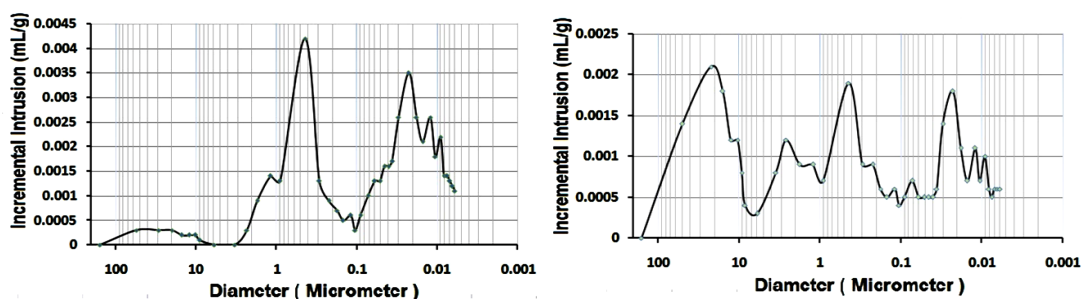


Figure 3. Incremental intrusion versus diameter for specimens of concrete (left: C0, right: N1).

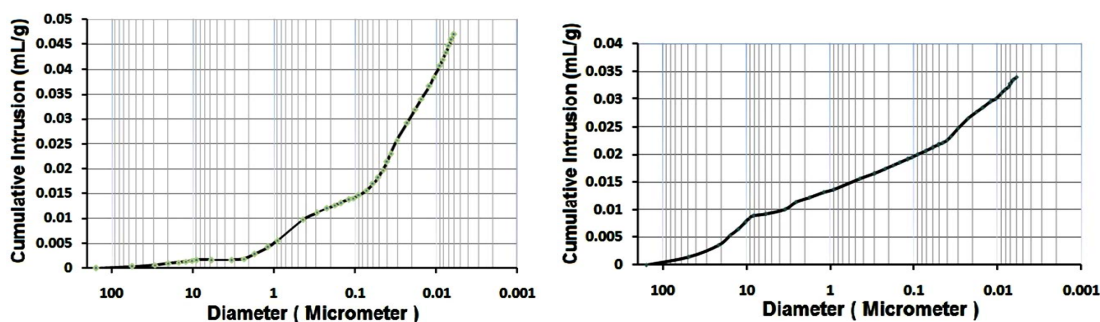


Figure 4. Cumulative intrusion versus diameter for specimens of concrete (left: C0, right: N1).

Table 6. Total intrusion volume, total pore area, median pore diameter (volume) and media pore diameter (area) of C0-SCC and N1-SCC specimens.

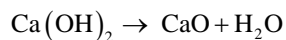
Sample name	Total intrusion volume/(mL/g)	Total pore area /(m ² /g)	Median pore diameter (volume)/nm	Median pore diameter (area)/nm
C0	0.048	8.48	35.1	10.4
N1	0.034	3.80	251.4	10.1

Table 7. Average pore diameter, bulk density, apparent (skeletal) density and porosity of C0-SCC and N1-SCC specimens.

Sample name	Average pore diameter/nm	Bulk density/(g/mL)	Apparent (skeletal) density/(g/mL)	Porosity/%
C0	22.2	2.64	3.02	12.40
N1	35.8	2.43	2.65	8.26

lume and the regularity of average pore diameter is similar to median diameter (volume). The increase of average pore diameter and median diameter (volume) are due to the ability of MnFe_2O_4 nanoparticles to fill the small pores. Also, the decrease of density is due to the replacement of cement by MnFe_2O_4 nanoparticles which have a lower density leading to a decrease in the density of the composite.

The thermal results of the C0-SCC specimen and N1-SCC specimen are shown in **Figure 5** which displays two lines. The solid line represents the thermogravimetric analysis and the dashed line represents the derivative thermogravimetry. It is clear that TGA curves for these pastes consist of three zones. The first weight loss zone usually includes capillary pore water, interlayer water and adsorbed water. The second weight loss zone includes dehydration of calcium silicate hydrates and the third zone includes the dehydration of CH. Following chemical reaction usually takes place in the third zone:



The TGA/DTG results clarify a reduction in the calcium hydroxide (CH) content in specimen N1-SCC compared to specimen C0-SCC which confirms the improvement of mechanical properties and occurrence of poz-

zolanitic reaction after 28 days of hydration.

Table 8 shows the thermogravimetric analysis results of C0-SCC and N1-SCC specimens measured to 650°C in which dehydration of the hydrated products occurred. The results show that after 28 days of curing, the loss in weight of the specimens is decreased by increasing MnFe_2O_4 nanoparticles in concretes by 0.5 wt%. The decrease in loss weight is due to more formation of C-S-H compounds in the cement paste [4].

Finally, **Figure 6** shows the SEM micrographs of C0-SCC specimen (control specimen) and N1-SCC specimen containing 0.5 wt% MnFe_2O_4 nanoparticles cured for 28 days. The morphological analysis of C0-SCC specimen shows clearly the presence of large pores. On the other hand, the morphological analysis shows that specimen reinforced with MnFe_2O_4 nanoparticles with 0.5 wt% is more compact and less porous in the paste with admixture than the control one. In spite of this, both reactions are observed to progress, with a considerable decrease in the amount of anhydrous cement particles which indicates rapid formation of C-S-H gel, especially in the presence of MnFe_2O_4 nanoparticles.

4. Conclusions

The obtained results can be summarized as follows:

- 1) The results showed that concrete specimen reinforced with MnFe_2O_4 nanoparticles had higher compressive strength compared to that of the concrete without MnFe_2O_4 nanoparticles. It was found that the cement could be advantageously doped with MnFe_2O_4 nanoparticles up to maximum limit of 1% by weight of cement

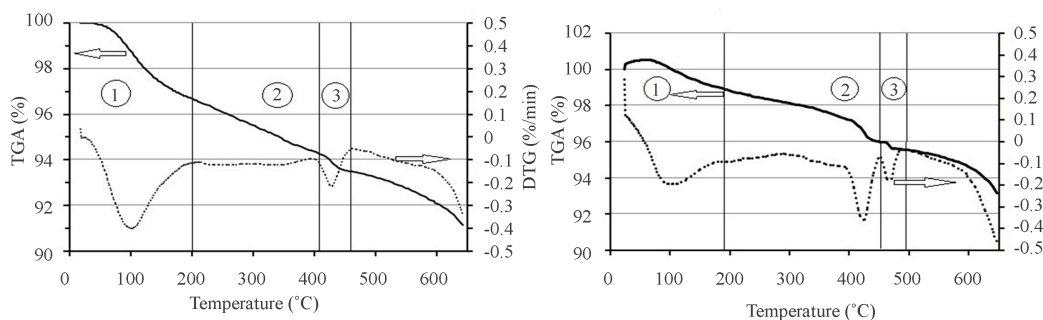


Figure 5. TGA /DTG profiles of specimens of concrete after 28 days of curing (left: C0, right: N1).

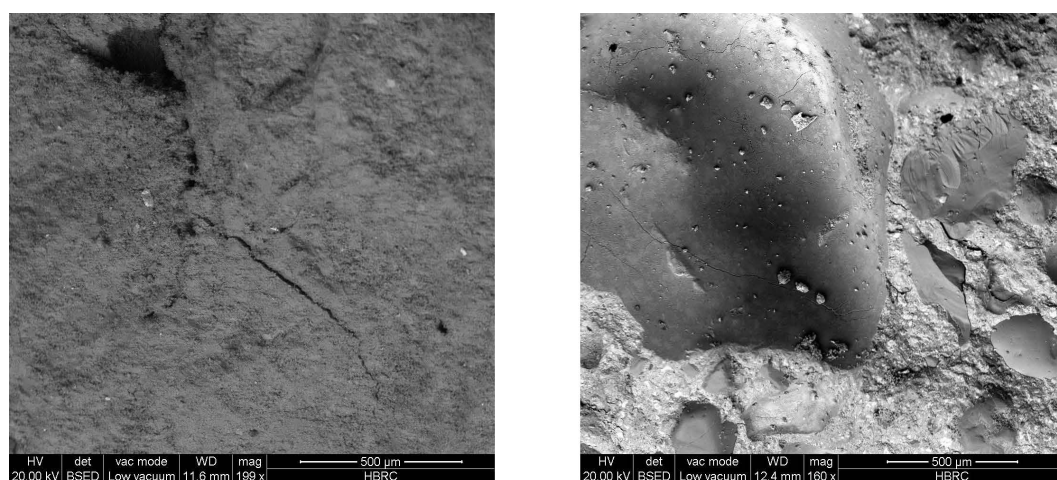


Figure 6. SEM micrograph of specimens of concrete after 28 days of curing (left: C0, right: N1).

Table 8. Weight loss (%) of the pastes in the range to 650°C after 28 days of curing of C0-SCC and N1-SCC specimens.

Sample name	Total weight loss/%
C0	8.77
N1	7.06

- with average diameter of 49 nm. However, the maximum value of compressive strength was achieved with 0.5 wt% doped MnFe₂O₄ nanoparticles. The addition of MnFe₂O₄ nanoparticles with 1.5 wt% and 2 wt% led to a compressive strength lower than the control specimen.
- 2) The pore structure of self-compacting concrete containing MnFe₂O₄ nanoparticles was improved and the volume of all mesopores and macropores was decreased.
 - 3) Thermogravimetric analysis showed that MnFe₂O₄ nanoparticles decreased the weight loss of the specimens when they were added to concrete with 0.5 wt%. More rapid formation of hydrated products in the presence of MnFe₂O₄ nanoparticles which was confirmed by these results could be the reason for minimizing weight loss.
 - 4) SEM images showed that specimen reinforced with MnFe₂O₄ nanoparticles with 0.5 wt% was more compact and less porous in the paste with admixture than the control one.

Acknowledgements

The authors would like to thank Dr. M. K. Abdelmaksoud and Dr. S. I. El-Dek for practical support in Materials Science Lab. (1), physics Department, Faculty of science, Cairo University, Giza, Egypt.

References

- [1] Soleymani, F. (2012) Computer-Aided Prediction of Physical and Mechanical Properties of High Strength Concrete Containing Fe₂O₃ Nanoparticles. *The Journal of American Science*, **8**, 338-345.
- [2] Tyson, B., Abu Al-Rub, R., Yazdanbakhsh, A. and Grasley, Z. (2011) Carbon Nanotubes and Carbon Nanofibers for Enhancing the Mechanical Properties of Nanocomposite Cementitious Materials. *Journal of Materials in Civil Engineering*, **23**, 1-8. [http://dx.doi.org/10.1061/\(ASCE\)MT.1943-5533.0000266](http://dx.doi.org/10.1061/(ASCE)MT.1943-5533.0000266)
- [3] Al-Salami, A.E., Al-Assiri, M.S., Al-Hajry, A., Ahmed, M.A. and Taha, S. (2007) The Effect of Curing Time and Porosity on the Microstructure Hydrated Products in Some Blended Cement Pastes. *Silicate Industrial*, **72**, 163.
- [4] Khoshakhlagh, A., Nazari, A. and Khalaj, G. (2012) Effects of Fe₂O₃ Nanoparticles on Water Permeability and Strength Assessments of High Strength Self-Compacting Concrete. *Journal of Materials Science Technology*, **28**, 73-82. [http://dx.doi.org/10.1016/S1005-0302\(12\)60026-7](http://dx.doi.org/10.1016/S1005-0302(12)60026-7)
- [5] Nazari, A. and Riahi, S. (2010) The Effects of ZrO₂ Nanoparticles on Physical and Mechanical Properties of High Strength Self Compacting Concrete. *Materials Research*, **13**, 551-556. <http://dx.doi.org/10.1590/S1516-14392010000400019>
- [6] Nazari, A., Riahi, S., Shamekhi, S. and Khademno, A. (2010) The Effects of Incorporation Fe₂O₃ Nanoparticles on Tensile and Flexural Strength of Concrete. *The Journal of American Science*, **6**, 90-93.
- [7] Nazari, A. and Riahi, S. (2011) Effects of CuO Nanoparticles on Compressive Strength of Self-Compacting Concrete. *Indian Academy of Sciences*, **36**, 371-391.
- [8] Chung, D.D.L. (2004) Cement-Matrix Structural Nanocomposites. *Metals and Materials*, **10**, 55-67. <http://dx.doi.org/10.1007/BF03027364>
- [9] British Standard Institution, BS 12 (1996) Specifications for Portland Cement. BSI, London.
- [10] Ahmed, M.A., Bishay, S.T. and El-Dek, S.I. (2012) Characteristics of Dy_{2.8}Sr_{0.2}Fe₅O₁₂ Garnet (DySrIG). *The European Physical Journal Applied Physics*, **59**, Article No. 20401. <http://dx.doi.org/10.1051/epjap/2012110465>
- [11] Ahmed, M.A., Okasha, N. and El-Dek, S.I. (2008) Preparation and Characterization of Nanometric Mn Ferrite via Different Methods. *Nanotechnology*, **19**, 6. <http://dx.doi.org/10.1088/0957-4484/19/6/065603>
- [12] ASTM C39 (2001) Standard Test Method for Compressive Strength of Cylindrical Concrete Specimens. ASTM, Philadelphia.
- [13] Abell, A., Willis, K. and Lange, D. (1999) Mercury Intrusion Porosimetry and Image Analysis of Cement-Based Materials. *Journal of Colloid and Interface Science*, **211**, 39. <http://dx.doi.org/10.1006/jcis.1998.5986>
- [14] Tanaka, K. and Kurumisawa, K. (2002) Development of Technique for Observing Pores in Hardened Cement Paste. *Cement and Concrete Research*, **32**, 1435. [http://dx.doi.org/10.1016/S0008-8846\(02\)00806-2](http://dx.doi.org/10.1016/S0008-8846(02)00806-2)
- [15] Yazdi, N., Arefi, M., Mollaahmadi, E. and Nejand, B. (2011) To Study the Effect of Adding Fe₂O₃ Nanoparticles on the Morphology Properties and Microstructure of Cement Mortar. *Life Science Journal*, **8**.
- [16] Li, H., Zhang, M.H. and Ou, J.P. (2006) Abrasion Resistance of Concrete Containing Nano-Particles for Pavement. *Wear*, **260**, 1262-1266. <http://dx.doi.org/10.1016/j.wear.2005.08.006>
- [17] Meng, T., Yu, Y., Qian, X., Zhan, S. and Qian, K. (2012) Effect of Nano-TiO₂ on the Mechanical Properties of Cement Mortar. *Construction and Building Materials*, **29**, 241-245. <http://dx.doi.org/10.1016/j.conbuildmat.2011.10.047>